

1 **Host glutathione is required for *Rickettsia parkeri* to properly septate, avoid**  
2 **ubiquitylation, and survive in macrophages.**

3

4 Han Sun<sup>1</sup>, Anh Phuong Luu<sup>1</sup>, Meggie Danielson<sup>1</sup>, Thaomy T. Vo<sup>1</sup>, Thomas P. Burke<sup>1\*</sup>.

5

6 <sup>1</sup>Department of Microbiology and Molecular Medicine, School of Medicine, University of California,  
7 Irvine, CA 92617 USA.

8

9 \*Correspondence: tpburke@uci.edu.

10 **Summary**

11 Spotted fever group *Rickettsia* obligately reside in the cytosol where they parasitize over fifty  
12 metabolites from their hosts. However, the role for metabolite acquisition in pathogenesis remains  
13 unclear. Here, we find that depletion of the abundant low molecular weight thiol glutathione led to an  
14 impaired ability of *Rickettsia parkeri* to form plaques. Super-resolution microscopy revealed that  
15 glutathione depletion with buthionine sulfoximine (BSO) in endothelial or epithelial cells led to the  
16 formation of bacterial chains that increased in length over time. Chained bacteria had fewer actin-tails  
17 and were impeded for their ability to spread from cell to cell. Glutathione depletion also caused an  
18 increased frequency of colocalization between the bacterial surface and polyubiquitin. *R. parkeri* was  
19 significantly more restricted upon glutathione depletion in primary macrophages than in epithelial cells  
20 in a mechanism that avoided activating the inflammasome and the production of type I interferon.  
21 Together, these data suggest that host glutathione is critical for rickettsial septation, actin-based  
22 motility, avoiding ubiquitylation, and survival in immune cells.

23 **Introduction**

24 Spotted fever group (SFG) *Rickettsia* species are dangerous agents of disease in the United  
25 States and worldwide (1). SFG *R. rickettsii* is the causative agent of Rocky Mountain spotted fever  
26 (RMSF), a disease characterized by fever of over 104° F, maculopapular rash, severe headache, and  
27 in some cases death (2). Case-fatality rates for RMSF were as high as 65-80% prior to antibiotics (3)  
28 and can be fatal even after antibiotic treatment (4). The SFG pathogen *R. parkeri* is the causative agent  
29 of mild spotted fever disease in North and South America (5-7) and has a highly similar genome to *R.*  
30 *parkeri*, with some virulence genes containing >99% sequence alignment, with the major difference  
31 being a single 33.5 kb locus that is absent in *R. rickettsii* (5). *R. parkeri* rickettsiosis is characterized by  
32 a skin lesion (eschar) at the site of tick bite, fever of 103° F, rash, and headache (6, 7). Spotted fever  
33 has increased in incidence from approximately 500 cases in the year 2000 to 6,248 cases in 2017, and  
34 disease occurs in every state of the continental United States (1). Spotted fever and other tick-borne  
35 diseases are increasing in prevalence as the range of ticks expands, which may be fueled by climate  
36 change (8). The increasing incidence combined with difficulties in recognizing spotted fever clinically  
37 (9) illustrate a critical need to better understand molecular mechanisms of disease caused by SFG  
38 rickettsial pathogens.

39 *Rickettsia* and their close relatives are obligate to the host cell cytosol, where they parasitize  
40 over 50 nutrients (10, 11). *Rickettsia* have highly reduced genomes with degraded biosynthetic  
41 pathways, including loss of enzymes required for glycolysis and the tricarboxylic acid cycle, as well as  
42 biosynthesis of fatty acids, isoprenoids, vitamins, cofactors and amino acids, and the abundant low  
43 molecular weight thiol glutathione (5, 10, 12). Glutathione prevents oxidative damage by reducing  
44 reactive oxygen species (ROS), and it can also function as a cysteine source after conversion to  
45 methionine. S-glutathionylation of cysteine can function as a post-translational modification that alters  
46 protein activity. *Rickettsia* encode a conserved glutathione S-transferase, an enzyme that catalyzes the  
47 addition of glutathione to substrates (10, 12), however the role for glutathione in intracellular growth and  
48 pathogenesis remains unclear.

49       Glutathione is critical for pathogenesis of other phylogenetically distinct cytosol-dwelling  
50    pathogens, including *Listeria monocytogenes*, *Burkholderia pseudomallei* and *Francisella* species. An  
51    extracellular histidine kinase domain of *B. pseudomallei* binds glutathione initiate expression of type VI  
52    secretion system (13). Inhibition of glutathione synthesis by buthionine sulfoximine (BSO), which is a  
53    potent, specific, non-toxic, and irreversible inhibitor of  $\gamma$ -glutamylcysteine synthetase, blocks *B.*  
54    *pseudomallei* virulence gene expression and inhibits cell to cell spread (13). In the case of *Listeria*  
55    *monocytogenes*, the bacteria sense host methylgloxy, resulting in the bacterial production of  
56    glutathione that activates the master virulence gene regulator PrfA (14–16). In *Francisella* species,  
57    glutathione is imported and degraded as a sulfur source (17–19). Other pathogens, including  
58    *Streptococcus* species and *Hemophilus influenzae* co-opt host glutathione to defend against oxidative  
59    stress (20, 21). These studies support an emerging concept that glutathione plays important yet distinct  
60    roles in virulence of intracellular bacteria.

61       Here, we investigated the role for glutathione in the intracellular growth and survival of an  
62    obligate cytosolic pathogen, *R. parkeri*. We find that it is required for specific aspects of intracellular  
63    growth in epithelial and endothelial cells, including proper septation, actin-based motility, and avoiding  
64    ubiquitylation. We also observe that glutathione is significantly more important for *R. parkeri* survival in  
65    macrophages than in epithelial or endothelial cells. These findings establish a critical role for host  
66    glutathione in *Rickettsia* pathogenesis and contribute to an emerging paradigm that cytosol-dwelling  
67    bacterial pathogens sense the host reducing environment for specific aspects of virulence.

68

## 69    **Results**

### 70    **Glutathione is required for proper plaque formation and septation of *R. parkeri* in epithelial and** 71    **endothelial cells.**

72       To investigate the role for glutathione in *R. parkeri* pathogenesis, we depleted glutathione with  
73    BSO in Vero cells, which are primate epithelial cells that are highly permissive to infection and measured  
74    *R. parkeri* plaque formation at 7 days postinfection (dpi). To discriminate between any potential effects  
75    that BSO had on the bacteria versus on the host cells, BSO was added to Vero cells overnight, then

76 washed from the cells 30 mins prior to infection with *R. parkeri*. At 7 dpi, infected cells were fixed and  
77 stained with crystal violet. High multiplicities of infection (MOIs) caused host cell lysis, yet *R. parkeri*  
78 was >500-fold attenuated in its ability to form plaques at lower MOIs in BSO-treated cells (**Fig. 1A**). To  
79 determine if the anti-rickettsial effect was due to BSO acting on the host cells or potentially on the  
80 bacteria, *R. parkeri* was incubated with BSO prior to infection of untreated Vero cells. Incubation of *R.*  
81 *parkeri* with BSO did not affect PFUs as compared to untreated controls (**Fig. 1A**), suggesting that BSO  
82 was acting on the host cells and not on *R. parkeri* directly. These data suggest that *R. parkeri* requires  
83 host glutathione for plaque formation.

84 To better understand the mechanism by which glutathione is required for plaque formation, we  
85 analyzed infection with immunofluorescence microscopy. In Vero cells treated with BSO, *R. parkeri* had  
86 normal morphology early during infection (<24 h), but the bacteria had altered morphology as time  
87 increased. Doublet bacteria were significantly more prevalent at 24 hpi in BSO-treated cells, and from  
88 48-96 hpi the bacteria were observed in chains of 3, 4, and >4 bacteria (**Fig. 1B**). To better discern the  
89 morphology of *R. parkeri* in BSO-treated cells we next employed super-resolution microscopy. Airyscan  
90 confocal laser scanning microscopy revealed that many bacterial chains measured over 10  $\mu$ M in length  
91 (**Fig. 1C**). Moreover, distinct separation was observed within the chained bacteria, suggesting that the  
92 chaining was due to a defect in septation. In contrast, bacteria in untreated cells were >90% single rods  
93 throughout the infection that consistently measured ~1  $\mu$ M in length (**Fig. 1E**). This suggests that host  
94 glutathione is required for proper septation of *R. parkeri*.

95

96 **Glutathione is required for proper actin-based motility of *R. parkeri*.**

97 It remained unclear if host glutathione was required for actin-based motility, which is critical for  
98 cell-cell spread and contributes to plaque formation. *R. parkeri* undergoes two temporally distinct  
99 phases of actin-based motility, an early phase mediated by RickA that results in short, curly actin tails,  
100 and a later phase mediated by Sca2 that results in long tails and is the major mediator of cell-cell spread  
101 (22–25). We quantified the frequency of actin-tail formation and actin colocalization in untreated and  
102 glutathione depleted cells. At 30 mpi, BSO did not affect the frequency of absent actin, polar actin,

103 diffuse actin, curly tails, or straight tails as compared to untreated cells. At 48 hpi, chained bacteria in  
104 BSO-treated cells had observable actin tails but with reduced frequency as compared to untreated (**Fig.**  
105 **2C**). Polar actin was often observable within chains of bacteria, suggesting that these bacteria had  
106 defects in septation and were not filamentous with a shared cytosol (**Fig. 2B**). At 72 hpi, *R. parkeri* in  
107 BSO-treated cells were largely absent of actin, as compared to untreated cells (**Fig. 2 C**). Lastly, as  
108 many *Rickettsia* species target endothelial cells during systemic infection, we determined the effects of  
109 BSO on infected human microvascular endothelial cells (HMEC-1). Similar results were observed  
110 between in HMEC-1 cells as Vero cells, including defects in septation and actin-based motility (**Fig.**  
111 **2D**). These data demonstrate that host glutathione is required for proper actin-based motility of *R.*  
112 *parkeri* and suggest that defects in cell-to-cell spread in BSO-treated cells may contribute to the inability  
113 of *R. parkeri* to form plaques.

114

115 **Glutathione depletion restricts *R. parkeri* in macrophages but does not cause significantly**  
116 **enhanced inflammasome activation or interferon production.**

117 Many spotted fever group *Rickettsia* associate with leukocytes throughout their infectious  
118 lifecycles, including macrophages and neutrophils in the skin and in internal organs upon dissemination  
119 (7, 26–29). We therefore sought to determine if glutathione was required for *R. parkeri* survival in  
120 primary macrophages. In bone marrow-derived macrophages (BMDMs), depletion of glutathione with  
121 BSO led to a reduction in recoverable PFUs that was more severe than in epithelial cells (**Fig. 3A**). The  
122 loss of recoverable PFUs could be due to either bacterial restriction or alternatively due to an inability  
123 of surviving bacteria to form plaques in the PFU assay. To discriminate between these possibilities, we  
124 analyzed infected BMDMs with immunofluorescence microscopy. This revealed that *R. parkeri* was  
125 largely absent from BMDMs at 48 hpi (**Fig. 3B**), suggesting that glutathione was essential for survival  
126 in macrophages.

127 It remained unclear if restriction in macrophages was the result of bacteriolysis. We previously  
128 described how lysis of *R. parkeri* in wild type (WT) macrophages by guanylate binding proteins (GBPs)  
129 leads to caspase 11 inflammasome activation and pyroptosis (30). However, in caspase 1 and 11

130 deficient BMDMs (*Casp1/11<sup>-/-</sup>*), killing of *R. parkeri* by GBPs instead releases DNA that activates the  
131 DNA sensor cGAS, causing release of type I interferon (IFN-I, (30)). To determine if glutathione is  
132 required for protecting against bacteriolysis, we measured host cell death in WT macrophages and IFN-  
133 I release in *Casp1/11<sup>-/-</sup>* macrophages in the presence or absence of BSO. In WT macrophages, BSO  
134 treatment resulted in similar LDH release than in untreated cells (Fig. 3C), suggesting that glutathione  
135 was not required for protecting against bacteriolysis. Infection of BSO-treated and untreated BMDMs  
136 resulted in similar amounts of IFN-I production in WT cells, while the amount of IFN-I production was  
137 reduced in BSO-treated *Casp1/11<sup>-/-</sup>* cells as compared to untreated cells (Fig. 3D). The explanation for  
138 reduced IFN-I in BSO-treated *Casp1/11<sup>-/-</sup>* is unclear, however this could be related to a stronger  
139 restriction of the bacteria, which we previously reported. Nevertheless, the lower IFN-I upon BSO-  
140 treatment suggests that glutathione depletion is not eliciting higher bacteriolysis and cGAS activation.  
141 Together, these data demonstrate that restriction of *R. parkeri* in macrophages is via a non-lytic  
142 mechanism that does not activate cytosolic pattern recognition receptors including caspase 11 or cGAS.  
143

144 **Host glutathione is required for *R. parkeri* to avoid targeting by ubiquitin.**

145 *R. parkeri* mutants that are unable to avoid targeting by ubiquitin are restricted in BMDMs but  
146 not in Vero cells (31, 32). Since restriction of *R. parkeri* by BSO in macrophages did not result in  
147 bacteriolysis, we hypothesized that restriction may involve ubiquitin-mediated restriction of the bacteria.  
148 We therefore examined whether glutathione depletion increased ubiquitin recruitment to *R. parkeri* in  
149 Vero cells and BMDMs. Immunofluorescence microscopy revealed that ~12% of the bacteria in BSO-  
150 treated Vero cells were positive for polyubiquitin, which was significantly more than the ~1% observed  
151 in untreated cells (Fig. 4A). These data demonstrate that host glutathione is required for *R. parkeri*  
152 avoidance of ubiquitylation and are aligned with our findings that restriction is via a non-bacteriolytic  
153 mechanism.

154

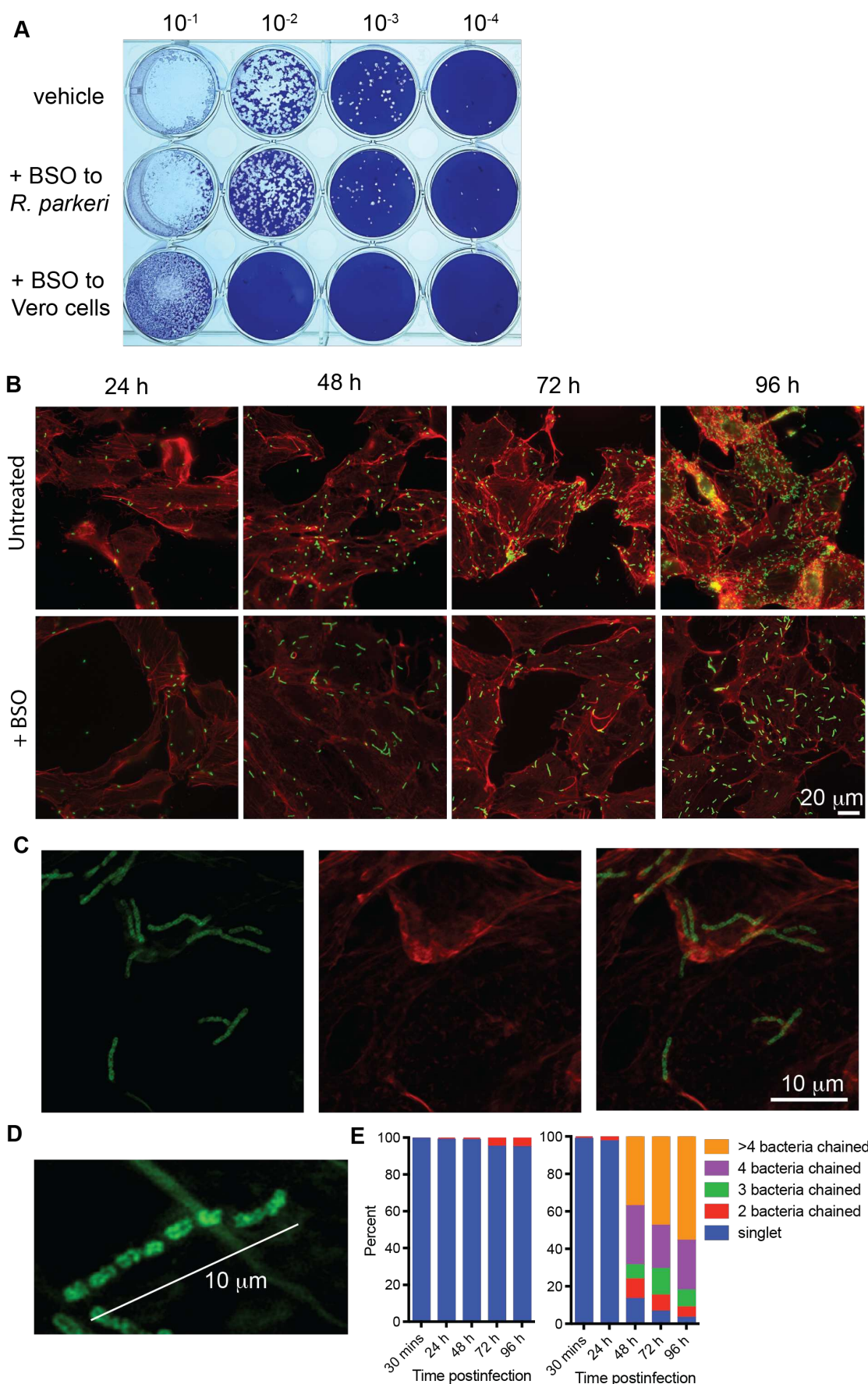
155 **Discussion**

156        Parasitizing metabolites from hosts is a critical aspect of pathogenesis for intracellular bacteria.  
157        As obligate intracellular pathogens, the *Rickettsia* steal over fifty host nutrients from their hosts and  
158        evolved a reduced genome size that has lost the ability to synthesize many metabolites *de novo*,  
159        including glutathione (10). In this study we find that host glutathione is required for *R. parkeri* septation,  
160        actin-based motility, avoiding ubiquitylation, and survival in macrophages. This reveals that host  
161        glutathione plays a critical role in specific aspects of *R. parkeri* pathogenesis and add to a growing  
162        paradigm that the reducing environment of the cytosol is a virulence cue for bacteria that reside in this  
163        compartment.

164        Glutathione is an abundant reducing agent of the host cytosol that can detoxify reactive oxygen  
165        species, alter proteins post-translationally, and be used as a cysteine source. Glutathione is used as a  
166        cue for *Burkholderia* to initiate virulence, whereby the extracellular domain of the histidine kinase VirA  
167        is reduced by glutathione, breaking it from a dimer to a monomer and resulting in transcription of the  
168        type VI secretion system (13). Additionally, *Listeria* senses the host reducing environment, synthesizes  
169        its own glutathione that post-translationally activates the master virulence transcription factor PrfA (14,  
170        15). Our findings reveal that host glutathione contributes *R. parkeri* pathogenesis, which could be  
171        mediated through either direct post-translational modification of factors involved in septation, or through  
172        virulence gene expression.

173        These observations across multiple phylogenetically distinct species suggests a paradigm that  
174        glutathione is a host-associated molecular pattern (HAMP) that is sensed by cytosolic microbes for  
175        virulence. We propose that the concept of HAMPs is similar to but on the opposite side of the coin as  
176        PAMPs (pathogen-associated molecular patterns). PAMPs are conserved molecular features of  
177        pathogens, such as flagellin, lipopolysaccharide, lipoproteins, and cyclic dinucleotides that are sensed  
178        by host cells as a signature of infection. Detection of PAMPs by host pattern recognition receptors  
179        (PRRs) leads to a host defense response such as upregulation of antimicrobial genes and programmed  
180        cell death. PAMPs and PRRs are well characterized; however, HAMPs are less well understood.  
181        Pathogens that reside directly in the cytosol such as *Rickettsia*, *Listeria*, *Burkholderia*, *Shigella* species,  
182        and *Mycobacterium marinum*, are ideal systems to study HAMPs because they initiate actin-based

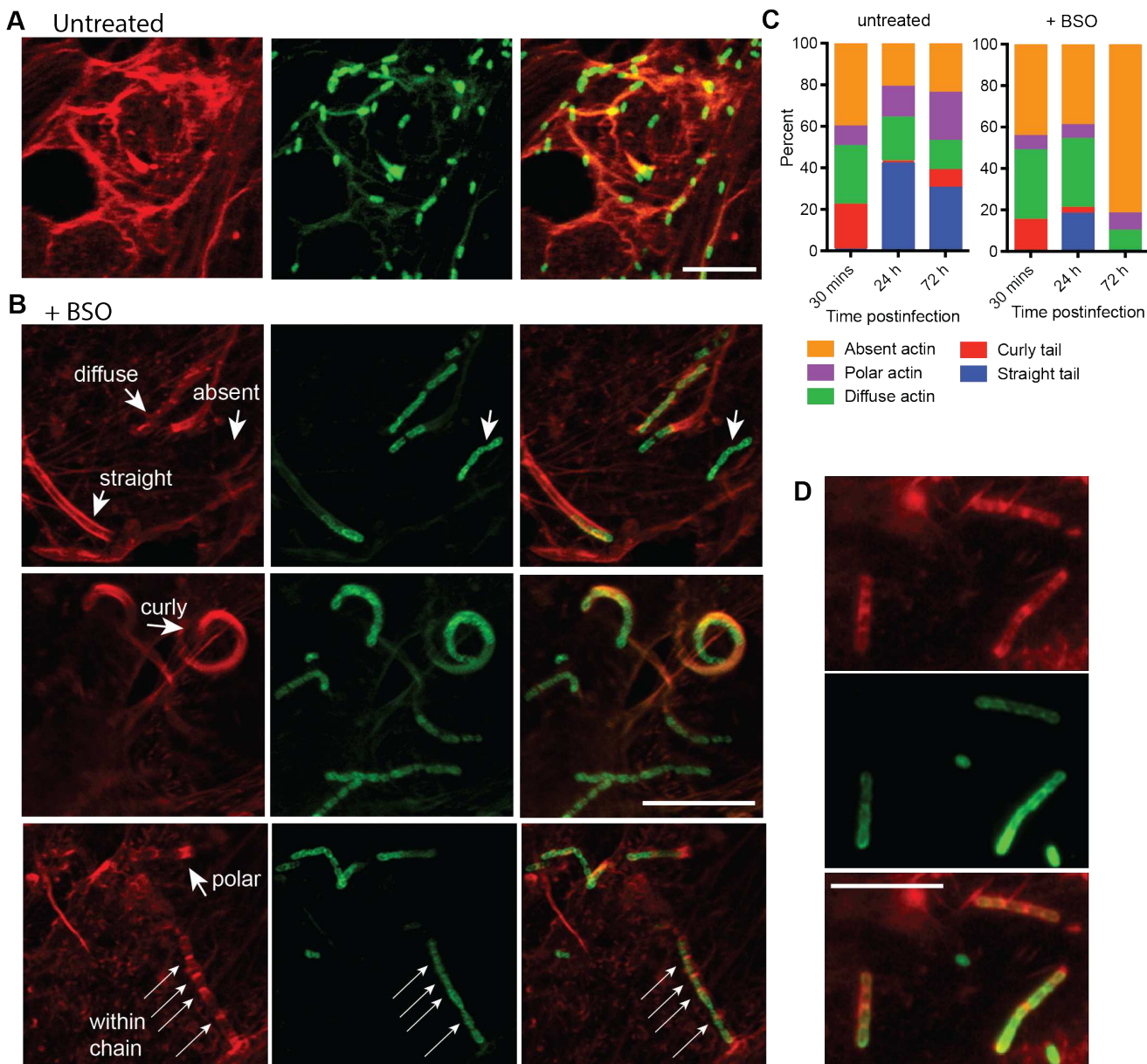
183 motility and other virulence genes only upon cytosolic entry. Identifying other HAMPs will increase our  
184 understanding of bacterial pathogenesis and potentially lead to new strategies for therapeutic targeting.



186 **Fig. 1: Glutathione is required for proper plaque formation and septation of *R. parkeri* in**  
187 **endothelial and epithelial cells.**

188 **A)** Vero cells were infected with *R. parkeri* at the indicated dilutions. For treatment of Vero cells, 2 mM  
189 BSO was added 16 h prior to infection, removed during infection, and added 30 again at mpi. For  
190 treatment of *R. parkeri*, bacteria were treated on ice for 15 m prior to infection with 2 mM BSO. Avicel  
191 was added at 24 hpi and cells were fixed at 7 dpi for crystal violet staining. Image is representative of  
192 three independent experiments. **B)** Representative immunofluorescence microscopy images of Vero  
193 cells infected with *R. parkeri* on coverslips in 24 well plates. **C,D)** Representative images of 63x confocal  
194 super-resolution microscopy of Vero cells treated with 2 mM BSO and infected with *R. parkeri*, at 48  
195 hpi. For all panels, cells were infected at an MOI of 1 and fixed with 4% paraformaldehyde at the  
196 indicated times. Coverslips were then stained with phalloidin (red) and with an anti-*Rickettsia* antibody  
197 (green). **E)** Quantification of images from HMEC-1 cells. Data are representative of at least three  
198 separate experiments.

199  
200  
201  
202



203

204

**Fig. 2: Host glutathione is required for proper actin-based motility of *R. parkeri*.**

205

206

207

208

209

210

211

212

213

214

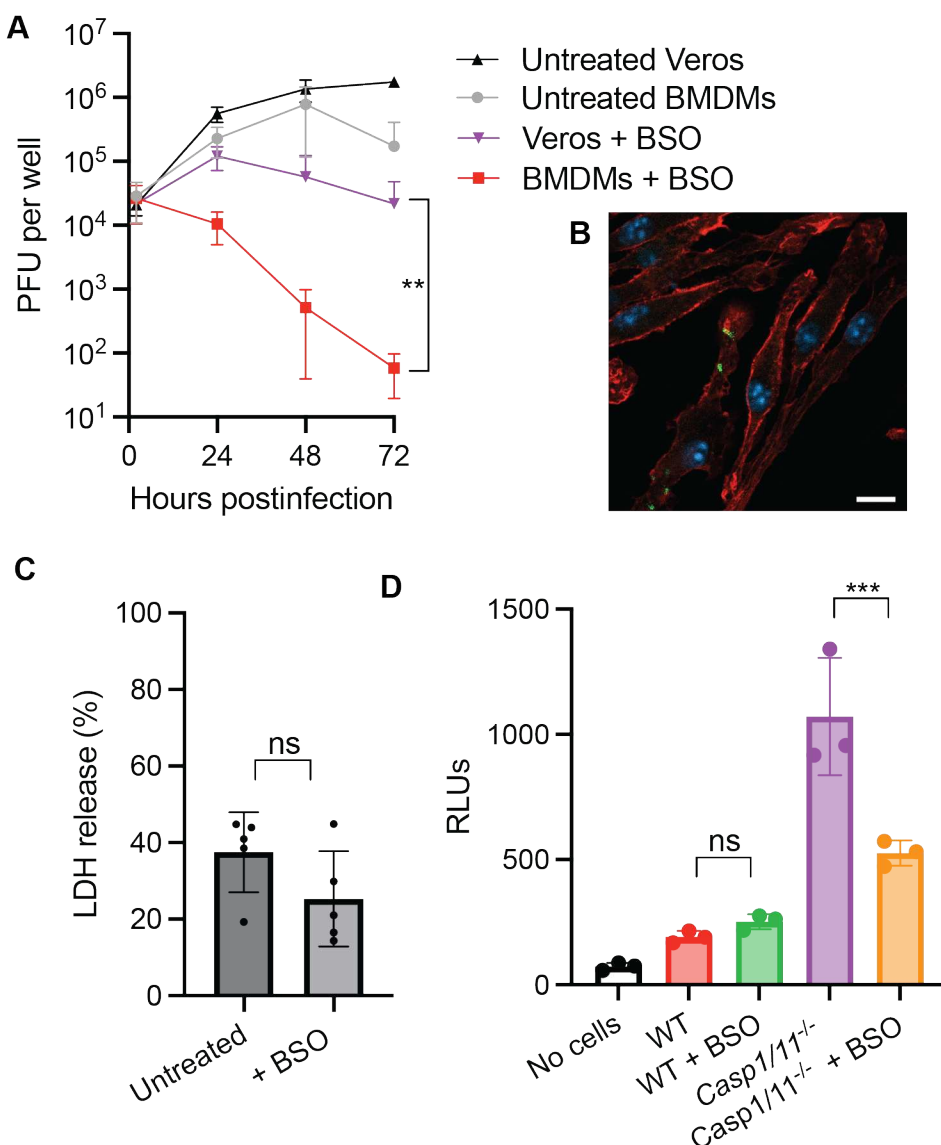
215

216

217

218

**A**) Representative images using 20x confocal immunofluorescence microscopy of Vero cells infected with *R. parkeri* at an MOI of 1 and imaged at 48 hpi. Scale bar = 10  $\mu$ m. **B**) Representative images using 63x confocal immunofluorescence microscopy of Vero cells infected with *R. parkeri* at an MOI of 1 and imaged at 48 hpi. 2 mM BSO was added prior to infection overnight. Scale bar = 10  $\mu$ m. **C**) Quantification of actin colocalization around *R. parkeri*. Each time point is an average of at least 4 separate experiments totaling >1,000 bacteria. **D**) Representative images of HMEC-1 cells treated with 2 mM BSO overnight and infected with *R. parkeri*, with 63x confocal microscopy at 48 hpi. For all microscopy experiments, coverslips containing infected cells were fixed with 4% PFA and stained with phalloidin (red), anti-*Rickettsia* (green). Data represent 3 independent experiments.



219

220

221

222

223

224

225

226

227

228

229

230

231

232

233

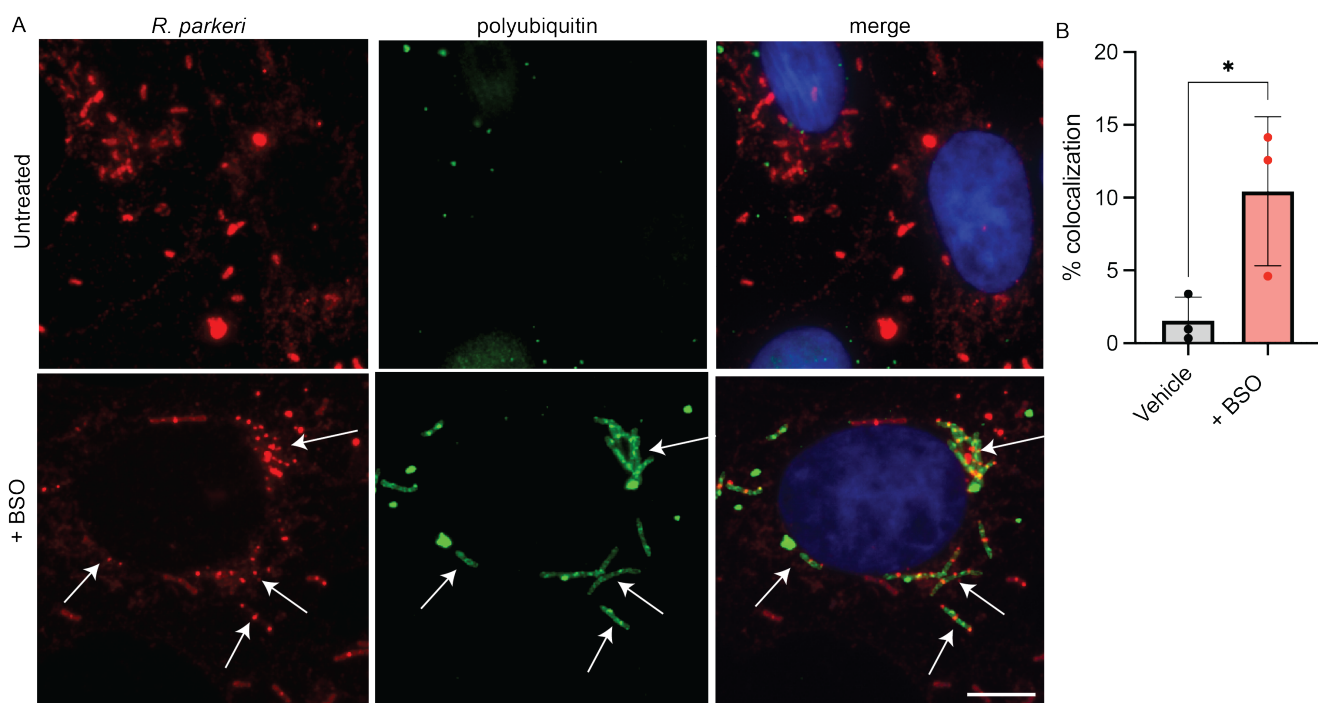
234

235

236

**Fig. 3: Host glutathione is required for *R. parkeri* survival in macrophages via a non-bacteriolytic restriction mechanism.**

A) *R. parkeri* abundance WT murine BMDMs or Vero cells infected at an MOI of 1. Each data point is the average of 3 independent experiments. Bars denote SD. Statistics used a two-way ANOVA. B) Representative images using 60x confocal microscopy of BMDMs treated with 2 mM BSO overnight, infected with *R. parkeri* at an MOI of 1 and imaged at 48 hpi. C) Quantification of host cell death during *R. parkeri* infection of WT BMDMs. LDH release was measured at 24 hpi upon *R. parkeri* infection at an MOI of 1. Data are the compilation of three separate experiments and are expressed as means  $\pm$  SD. Statistical analyses in used a two-tailed Student's T test. D) Measurement of IFN- $\beta$  in supernatants of BMDMs infected with *R. parkeri* at an MOI of 1. Supernatants were harvested at 24 hpi and used to stimulate a luciferase-expressing cell line (ISRE) and relative light units (RLU) were measured and compared between treated and untreated cells. Statistical comparisons were made use a Student's two-way T-Test. Data are the compilation of three separate experiments and are expressed as means  $\pm$  SD. \*\*p<0.01, ns=not significant.



237

238

**Fig. 4: Host glutathione is required for *R. parkeri* to avoid ubiquitylation.**

239

240

241

242

243

244

245

246

A) Representative images of ubiquitin colocalization using immunofluorescence microscopy of Vero cells infected with *R. parkeri* at an MOI of 1 and fixed at 48 hpi. Cells treated with 2 mM BSO were incubated overnight with the drug. Cells were stained with FK1 anti-polyubiquitin (green), anti-*Rickettsia* I7 (red); and DAPI (blue). Scale bar = 10  $\mu$ m. B) Quantification of ubiquitin colocalization at 48 hpi in Vero cells. Each data point is an independent experiment with at least 4 images and each image contained at least 50 bacteria. Data are expressed as means  $\pm$  SD. Statistical analysis used a two-tailed Student's T test; \*p<0.05.

247

## Methods

248

### Preparation of *R. parkeri*

249

250

251

252

253

254

255

256

257

*R. parkeri* strain Portsmouth was originally obtained from Christopher Paddock (Centers for Disease Control and Prevention). Bacteria were amplified by infecting confluent T175 flasks of female African green monkey kidney epithelial Vero cells were obtained from the UC Berkeley Cell Culture Facility, where they were tested for mycoplasma contamination, and were authenticated by mass spectrometry experiments. Vero cells were grown in DMEM (Gibco 11965-092) with glucose (4.5 g/L) supplemented with 2% fetal bovine serum (FBS, GemCell) with  $5 \times 10^6$  *R. parkeri* per flask. Infected cells were scraped and collected at 5 dpi when ~90% of cells were highly infected. Scrapped cells were centrifuged at 12,000 x G for 20 min at 4°C. Pelleted cells were then resuspended in K-36 buffer (0.05 M KH<sub>2</sub>PO<sub>4</sub>, 0.05 M K<sub>2</sub>HPO<sub>4</sub>, 100 mM KCl, 15 mM NaCl, pH 7) and dounced (60 strokes) at 4°C. The

258 solution was then centrifuged at 200 x G for 5 min at 4°C to pellet host cell debris. Supernatant  
259 containing *R. parkeri* was overlaid on a 30% MD-76R (Merry X-Ray) solution. Gradients were  
260 centrifuged at 18,000 rpm in an SW-28 ultracentrifuge swinging bucket rotor (Beckman/Coulter) for 20  
261 min at 4°C to separate host cells debris. Bacterial pellets were resuspended in brain heart infusion (BHI)  
262 media (BD, 237500) and stored at -80°C.

263 Titors were determined via plaque assays by serially diluting the bacteria in 6-well plates  
264 containing confluent Vero cells. Plates were then spun for 5 min at 300 x G in an Eppendorf 5810R  
265 centrifuge. At 24 hpi, the media from each well was aspirated and the wells were overlaid with 4 ml/well  
266 DMEM with 5% FBS and 0.7% agarose (Invitrogen, 16500-500). At 7 dpi, cells were fixed, stained, and  
267 counted as described below.

268

269 **Deriving bone marrow macrophages**

270 To obtain bone marrow, male or female mice were euthanized, and femurs, tibias, and fibulas  
271 were excised. Connective tissue was removed, and the bones were sterilized with 70% ethanol. Bones  
272 were washed with BMDM media (20% HyClone FBS, 1% sodium pyruvate, 0.1%  $\beta$ -mercaptoethanol,  
273 10% conditioned supernatant from 3T3 fibroblasts, in Gibco DMEM containing glucose and 100 U/ml  
274 penicillin and 100 ug/ml streptomycin) and ground using a mortar and pestle. Bone homogenate was  
275 passed through a 70  $\mu$ m nylon Corning Falcon cell strainer (Thermo Fisher Scientific, 08-771-2) to  
276 remove particulates. Filtrates were centrifuged in an Eppendorf 5810R at 1,200 RPM (290 x G) for 8  
277 min, supernatant was aspirated, and the remaining pellet was resuspended in BMDM media. Cells were  
278 then plated in non-TC-treated 15 cm petri dishes (at a ratio of 10 dishes per 2 femurs/tibias) in 30 ml  
279 BMDM media and incubated at 37° C. An additional 30 ml was added 3 d later. At 7 d the media was  
280 aspirated, and cells were incubated at 4°C with 15 ml cold PBS (Gibco, 10010-023) for 10 min. BMDMs  
281 were then scraped from the plate, collected in a 50 ml conical tube, and centrifuged at 1,200 RPM (290  
282 x G) for 5 min. The PBS was then aspirated, and cells were resuspended in BMDM media with 30%  
283 FBS and 10% DMSO at  $10^7$  cells/ml. 1 ml aliquots were stored in liquid nitrogen.

284

285 **Infections *in vitro***

286 To plate cells for infection, aliquots of BMDMs were thawed on ice, diluted into 9 ml of DMEM,  
287 centrifuged in an Eppendorf 5810R at 1,200 RPM (290 x G) for 5 minutes, and the pellet was  
288 resuspended in 10 ml BMDM media without antibiotics. The number of cells was counted using Trypan  
289 blue (Sigma, T8154) and a hemocytometer (Bright-Line), and  $5 \times 10^5$  cells were plated into 24-well  
290 plates. Approximately 16 h later, 30% prep *R. parkeri* were thawed on ice and diluted into fresh BMDM  
291 media to the desired concentration (either  $10^6$  PFU/ml or  $2 \times 10^5$  PFU/ml). Media was then aspirated from  
292 the BMDMs, replaced with 500  $\mu$ l media containing *R. parkeri*, and plates were spun at 300 G for 5 min  
293 in an Eppendorf 5810R. Infected cells were then incubated in a humidified CEDCO 1600 incubator set  
294 to 33°C and 5% CO<sub>2</sub> for the duration of the experiment. For treatments with recombinant mouse IFN- $\beta$ ,  
295 IFN- $\beta$  (PBL, 12405-1) was added directly to infected cells immediately after spinfection. L-BSO was  
296 obtained from Sigma (B2515).

297 Titters were determined via plaque assays by serially diluting the bacteria in 12-well plates  
298 containing confluent Vero cells. Plates were then spun for 5 min at 300 x G in an Eppendorf 5810R  
299 centrifuge. At 24 hpi, the media from each well was aspirated and the wells were overlaid with 2 mL/well  
300 DMEM with 5% FBS and 1.2% Avicel® PH-101 (Sigma, 11363). At 7 dpi, the wells were overlaid with 2  
301 mL/well of 7% Formaldehyde (VWR, 10790-708) for 30 minutes. Media was then aspirated, and the  
302 wells were stained with 0.5 mL/well of 1x Crystal Violet (VWR, 470337-534) for 15 minutes. Crystal  
303 Violet was then washed off using DI water and plaques were counted 24h later.

304

305 **Microscopy**

306 For immunofluorescence microscopy,  $2.5 \times 10^5$  Vero, HMEC-1, or BMDMs were plated overnight  
307 in 24-well plates with sterile 12 mm coverslips (Thermo Fisher Scientific, 12-545-80). Infections were  
308 performed as described above. At the indicated times post-infection, coverslips were washed once with  
309 PBS and fixed in 4% paraformaldehyde (Ted Pella Inc., 18505, diluted in 1 x PBS) for 10 min at room  
310 temperature. Coverslips were then washed 3 times in PBS. Coverslips were washed once in blocking  
311 buffer (1 x PBS with 2% BSA) and permeabilized with 0.5% triton X-100 for 10 min. Coverslips were

312 incubated with antibodies diluted in 2% BSA in PBS for 30 min at room temperature. *R. parkeri* was  
313 detected using mouse anti-*Rickettsia* 14-13 or I7 (originally from Dr. Ted Hackstadt, NIH/NIAID Rocky  
314 Mountain Laboratories). Polyubiquitin was stained the FK1 antibody (Novus). Nuclei were stained with  
315 DAPI, and actin was stained with Alexa-568 phalloidin (Life Technologies, A12380). Secondary  
316 antibodies were Alexa-405 goat anti-mouse (A31553) and Alexa-488 goat anti-rabbit (A11008).  
317 Coverslips were mounted in Prolong mounting media (Invitrogen). Samples were imaged with either the  
318 Keyence BZ-X810 Inverted Microscope with 20x or a 60x oil objective or the Airyscan 2/ GaAsP function  
319 of the Zeiss LSM 900 Confocal Multiplex with Plan-Apochromat 63x/1.4 Oil DIC M27 (FWD=0.19mm)  
320 objective or the Plan-Apochromat 20x/0.8 M27 (FWD=0.55mm) objective at the UC Irvine Microscope  
321 Imaging Core. Images were processed using FIJI<sup>49</sup> and brightness and contrast adjustments were  
322 applied to entire images. Images were assembled using Adobe Illustrator. Representative images are  
323 a single optical section.

324

325 ***In vitro* assays**

326 For LDH assays, 60  $\mu$ l of supernatant from wells containing BMDMs was collected into 96-well  
327 plates. 60  $\mu$ l of LDH buffer was then added. LDH buffer contained: 3  $\mu$ l of "INT" solution containing 2  
328 mg/ml tetrazolium salt (Sigma I8377) in PBS; 3  $\mu$ l of "DIA" solution containing 13.5 units/ml diaphorase  
329 (Sigma, D5540), 3 mg/ml  $\beta$ -nicotinamide adenine dinucleotide hydrate (Sigma, N3014), 0.03% BSA,  
330 and 1.2% sucrose; 34  $\mu$ l PBS with 0.5% BSA; and 20  $\mu$ l solution containing 36 mg/ml lithium lactate in  
331 10 mM Tris HCl pH 8.5 (Sigma L2250). Supernatant from uninfected cells and from cells completely  
332 lysed with 1% triton X-100 (final concentration) were used as controls. Reactions were incubated at  
333 room temperature for 20 min prior to reading at 490 nm using an Infinite F200 Pro plate reader (Tecan).  
334 Values for uninfected cells were subtracted from the experimental values, divided by the difference of  
335 triton-lysed and uninfected cells, and multiplied by 100 to obtain percent lysis. Each experiment was  
336 performed and averaged between technical duplicates and biological triplicates.

337 For the IFN-I bioassay, 5  $\times$  10<sup>4</sup> 3T3 cells containing an interferon-sensitive response element  
338 (ISRE) fused to luciferase<sup>51</sup> were plated per well into 96-well white-bottom plates (Greneir 655083) in

339 DMEM containing 10% FBS, 100 U/ml penicillin and 100 µg/ml streptomycin. Media was replaced 24 h  
340 later and confluent cells were treated with 2 µl of supernatant harvested from BMDM experiments.  
341 Media was removed 4 h later and cells were lysed with 40 µl TNT lysis buffer (20 mM Tris, pH 8, 200  
342 mM NaCl, 1% triton-100). Lysates were then injected with 40 µl firefly luciferin substrate (Biosynth) and  
343 luminescence was measured using a SpectraMax L plate reader (Molecular Devices).

344

345 **Statistical analysis**

346 Statistical parameters and significance are reported in the Figure legends. For comparing two  
347 sets of data, a two-tailed Student's T test was performed. For comparing multiple data sets, a one-way  
348 ANOVA with multiple comparisons with Tukey post-hoc test was used for normal distributions, and a  
349 Mann-Whitney *U* test was used for non-normal distributions. Data are determined to be statistically  
350 significant when  $p<0.05$ . All data points shown in bar graphs and in animal data are distinct samples.  
351 Asterisks denote statistical significance as: \*,  $p<0.05$ ; \*\*,  $p<0.01$ ; \*\*\*,  $p<0.001$ ; \*\*\*\*,  $p<0.0001$ , compared  
352 to indicated controls. For animal experiments, bars denote medians. Error bars indicate standard  
353 deviation (SD). All other graphical representations are described in the Figure legends. Statistical  
354 analyses were performed using GraphPad PRISM.

355

356 **Data availability**

357 *R. parkeri* strains were authenticated by whole genome sequencing and are available in the  
358 NCBI Trace and Short-Read Archive; Sequence Read Archive (SRA), accession number SRX4401164.

359

360

361

362 **References**

363

364 **Additional Information**

365 Correspondence and requests for materials should be addressed to T.P.B.

366

367 **Competing interests**

368 The authors declare no competing interests.

369

370 **Author contributions**

371 H.S., T.T.V, M.D., A.P.L, and T.P.B. performed and analyzed *in vitro* and *in vivo* experiments.

372 T.P.B. wrote the original draft of this manuscript. Critical reading and further edits were also provided

373 by H.S., M.D., and A.P.L. Supervision was provided by T.P.B.